Ruthenium(II) Complexes of *closo*-Dodecaboranyl Anions and the Molecular Structure of the *pileo*† Thirteen-vertex Ruthenaborane $[(PPh_3)_2ClRuB_{12}H_{11}(NEt_3)]$‡

Margaret Elrington, Norman N. Greenwood, John D. Kennedy, and Mark Thornton-Pett
Department of Inorganic and Structural Chemistry, The University of Leeds, Leeds LS2 9JT

Reaction of $Na_2[closo\text{-}B_{12}H_{12}]$ with $[RuCl_3(PMe_2Ph)_3]$ gives a 10% yield of the lemon-yellow air-stable covalent complex $[(PMe_2Ph)_3RuB_{12}H_{12}]$, characterized by elemental analysis and multi-element nuclear magnetic single- and multiple-resonance spectroscopy. Reaction of $[NHEt_3]_2[B_{12}H_{12}]$ and $[RuCl_2(PPh_3)_3]$ results in the formation of $[(PPh_3)_2ClRuB_{12}H_{11}(NEt_3)]$ as an orange-red air-stable compound (30%), characterized by single-crystal *X*-ray diffraction analysis as well as n.m.r. spectroscopy. The solvate $[(PPh_3)_2ClRuB_{12}H_{11}(NEt_3)]\cdot CH_2Cl_2$ forms monoclinic crystals, with a = 2 246.3(2), b = 1 189.2(2), c = 1 972.5(2) pm, β = 111.04(1)°, Z = 4, and space group $P2_1/n$. The compounds may formally be regarded either as ruthenium(II) complexes of *closo*-dodecaboranyl ligands which bind in a trihapto tridentate mode to the octahedral metal centres *via* three two-electron three-centre B–H–Ru bridge bonds, or as 13-vertex *pileo* 2*n*-electron metallaborane cluster species which have capped closed deltahedral cluster geometries.

The *closo*-$[B_{10}H_{10}]^{2-}$ anion readily forms complexes with transition-metal centres such as those containing copper [1–3] and platinum.[4] In these compounds the *closo* structure of the borane ligand is retained, and it is bound to the metal centre *via* its *exo* hydrogen atoms which, to a first approximation,[2] partake in two-electron three-centre B–H–M bridge bonding. Although this mode of bonding is in principle available to other *closo*-borane anions, a comprehensive survey [5] of metallaborane structural types reveals no further examples. Here we now report the isolation and characterization of complexes of the 12-vertex *closo*-borane anions $[B_{12}H_{12}]^{2-}$ and $[B_{12}H_{11}(NEt_3)]^-$ with triorganophosphine-substituted ruthenium(II) centres. Our attention to this new chemistry was initially attracted by the presence of these products in small amounts in ruthenium reaction systems that used the 10-vertex *closo*-$[B_{10}H_{10}]^{2-}$ anion as a starting substrate,[6–8] but in which the borane starting material was contaminated with small amounts of $[B_{12}H_{12}]^{2-}$ as an impurity which we had previously presumed was inert in this type of system.

Results and Discussion

The reaction between $Na_2[B_{12}H_{12}]$ and $[RuCl_3(PMe_2Ph)_3]$ in refluxing ethanol for 1 h, followed by chromatographic separation of the products, results in a 10% yield of a lemon-yellow microcrystalline air-stable solid. Analytical and n.m.r. data for this product are consistent with the formulation $[(PMe_2Ph)_3RuB_{12}H_{12}]$. From this formulation it is apparent that a reduction from ruthenium(III) to ruthenium(II) has occurred, and so the reaction is more complex than a straightforward stoicheiometric substitution. This is presumably reflected in the low yield [contrast the reaction of equation (1) below].

The gross geometry of the complex readily follows from the cluster n.m.r. properties (Table 1 and Figure 1). The similarity of the ^{11}B chemical shifts to that of the uncomplexed $[B_{12}H_{12}]^{2-}$ anion [$\delta(^{11}B)$ *ca.* −16 p.p.m. in CD_2Cl_2 solution] [9] indicates that the *closo*-dodecaboranyl bonding and geometric character

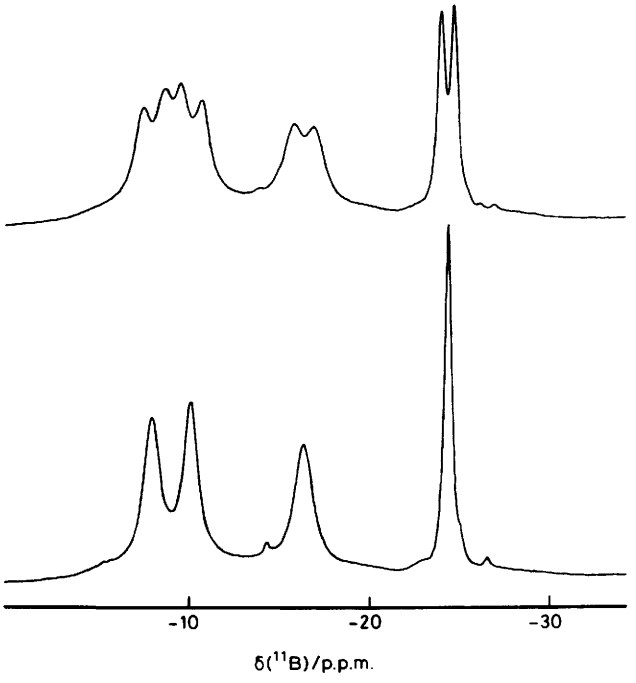

Figure 1. 115.5-MHz ^{11}B (upper trace) and ^{11}B-{^1H(broad-band noise)} (lower trace) n.m.r. spectra of $[(PMe_2Ph)_3RuB_{12}H_{12}]$ in CD_2Cl_2 solution at 21 °C

† We use the descriptor '*pileo*' (Latin: *pileus*, a brimless cap) to imply simple 2*n* cluster-electron counts and the exclusive geometries that clusters with such electron counts may adopt: '*pileo*' therefore has a similar usage to the descriptors '*closo*', '*nido*', '*arachno*', *etc.*, for cluster systems with, respectively, 2*n* + 2, 2*n* + 4, 2*n* + 6, *etc.*, cluster electrons. This usage releases the geometrical descriptor 'capped *closo*' (which would have inappropriate geometrical implications in the general case) for use in the purely geometric description of one of the configurations available to a system with a *pileo* electron count. It also avoids such terms as '*hypercloso*' and 'hyperdeficient' which are insufficiently precise and/or make presumptions about how many electrons it is thought that a cluster ought to have, which again may be inappropriate in the general case.

‡ Chloro[1—3-η-dodecahydro-7-triethylamine-*closo*-dodecaborato-(1 −)]bis(triphenylphosphine)ruthenium(II).

Supplementary data available: see Instructions for Authors, *J. Chem. Soc., Dalton Trans.*, 1987, Issue 1, pp. xvii—xx.

Table 1. Selected n.m.r. parameters for $[(PMe_2Ph)_3RuB_{12}H_{12}]$ in CD_2Cl_2 solution at 21 °C[a]

$\delta(^{11}B)$[b]	Relative intensity	$\delta(^1H)$[c]	Relative intensity	$^1J(^{11}B-^1H)$/Hz
−8.0	3 B	+2.05	3 H	*ca.* 135
−10.2	3 B	+1.82	3 H	*ca.* 140
−16.4	3 B	+1.77	3 H	*ca.* 130
−24.6[d]	3 B	−5.41[e]	3 H	*ca.* 80

[a] $\delta(^{31}P)$ +27.3 p.p.m. (−50 °C) relative to 85% H_3PO_4. [b] In p.p.m. ±0.5 to high field (low frequency) of $BF_3(OEt_2)$ in $CDCl_3$. [c] In p.p.m. ±0.05 to high field (low frequency) of $SiMe_4$ in CD_2Cl_2; proton resonances related to directly bound boron atoms by selective $^1H-\{^{11}B\}$ experiments. [d] B(1), B(2), B(3). [e] H(1), H(2), H(3) bridging atoms; doublet $^2J(^{31}P-Ru-^1H)$ (*trans*) *ca.* 25 Hz.

Table 2. Selected internuclear distances (pm) for $[(PPh_3)_2ClRuB_{12}H_{11}(NEt_3)]\cdot CH_2Cl_2$ with estimated standard deviations (e.s.d.s) in parentheses

(*i*) From the ruthenium atom

Ru(1)–P(1)	226.6(4)	Ru(1)–B(1)	226.9(12)
Ru(1)–P(2)	227.7(4)	Ru(1)–B(2)	248.4(12)
Ru(1)–Cl(1)	238.2(4)	Ru(1)–B(3)	245.0(12)

(*ii*) Interboron distances

B(1)–B(2)	173.2(16)	B(7)–B(2)	178.9(16)
B(2)–B(3)	176.7(16)	B(7)–B(3)	179.2(17)
B(3)–B(1)	174.0(16)	B(7)–B(8)	180.6(17)
		B(7)–B(11)	180.8(17)
Other B–B	175.1(17)—183.4(17)	B(7)–B(12)	178.4(17)
Mean of all B–B	178.9		

(*iii*) Other distances

B(6)–N(1)	163.1(15)	P(1)–C(111)	184.6(7)
N(1)–C, N(1)–C, N(1)–C	Disordered	P(1)–C(121)	185.1(7)
		P(1)–C(131)	184.3(7)
		P(2)–C(211)	183.2(7)
		P(2)–C(221)	183.6(7)
		P(2)–C(231)	187.0(7)

Table 3. Selected interatomic angles (°) for $[(PPh_3)_2ClRuB_{12}H_{11}(NEt_3)]\cdot CH_2Cl_2$, with e.s.d.s in parentheses

(*i*) About the ruthenium atom

P(1)–Ru(1)–P(2)	100.8(2)	Cl(1)–Ru(1)–B(1)	142.7(3)
P(1)–Ru(1)–Cl(1)	96.5(2)	Cl(1)–Ru(1)–B(2)	103.5(3)
P(1)–Ru(1)–B(1)	107.1(4)	Cl(1)–Ru(1)–B(3)	103.7(3)
P(1)–Ru(1)–B(2)	144.1(2)		
P(1)–Ru(1)–B(3)	104.5(4)	B(1)–Ru(1)–B(2)	42.4(3)
P(2)–Ru(1)–Cl(1)	93.6(2)	B(1)–Ru(1)–B(3)	43.1(3)
P(2)–Ru(1)–B(1)	109.3(4)	B(2)–Ru(1)–B(3)	42.0(3)
P(2)–Ru(1)–B(2)	107.3(3)		
P(2)–Ru(1)–B(3)	147.2(2)		

(*ii*) Ruthenium–boron–boron

B(2)–B(1)–Ru(1)	75.4(6)	B(7)–B(2)–Ru(1)	122.0(7)
B(3)–B(1)–Ru(1)	74.0(6)	B(11)–B(2)–Ru(1)	169.7(6)
B(4)–B(1)–Ru(1)	118.6(7)		
B(5)–B(1)–Ru(1)	172.1(7)	B(1)–B(3)–Ru(1)	62.9(6)
B(6)–B(1)–Ru(1)	122.2(7)	B(2)–B(3)–Ru(1)	70.1(6)
		B(4)–B(3)–Ru(1)	110.8(7)
B(1)–B(2)–Ru(1)	62.1(5)	B(7)–B(3)–Ru(1)	123.7(7)
B(3)–B(2)–Ru(1)	68.0(6)	B(8)–B(3)–Ru(1)	171.3(7)
B(6)–B(2)–Ru(1)	110.8(7)		

(*iii*) Carbon–phosphorus–ruthenium

C(111)–P(1)–Ru(1)	107.0(3)	C(211)–P(2)–Ru(1)	108.6(3)
C(121)–P(1)–Ru(1)	120.8(3)	C(221)–P(2)–Ru(1)	116.8(3)
C(131)–P(1)–Ru(1)	120.9(3)	C(231)–P(2)–Ru(1)	122.4(3)

(*iv*) Boron–boron–nitrogen

B(2)–B(7)–N(7)	122.5(9)	B(11)–B(7)–N(7)	120.1(9)
B(3)–B(7)–N(7)	124.4(9)	B(12)–B(7)–N(7)	121.7(9)
B(8)–B(7)–N(7)	122.2(9)		

(*v*) Boron–boron–boron

Average acute angle	60.0 [range 57.6(6)—61.4(7)]
Average obtuse angle	109.8 [range 103.6(8)—112.2(8)]

are still present, and the 3:3:3:3 intensity pattern suggests a metallaborane configuration in which a three-fold axis of the *closo*-B_{12} icosahedron is retained. Three of these four sets of boron sites are associated with *exo*-terminal hydrogen atoms which have proton chemical shifts $\delta(^1H)$ within normal ranges, but the fourth type of site is associated with proton shieldings some 7 p.p.m. to higher field of these, indicative of B–H–M bridge bonding.[9] This last three-proton resonance has a doublet splitting, presumably arising principally from couplings $^2J(^{31}P-Ru-^1H)$(*trans*) to each of the three equivalent phosphine ligands. The complex is therefore reasonably formulated as a complex of *closo*-$[B_{12}H_{12}]^{2-}$ in which the effective $[Ru(PMe_2Ph)_3]^{2+}$ metal centre is bound to the borane cluster *via* three equivalent Ru–H–B links, each of these links being *trans* to a ruthenium-bound PMe_2Ph ligand, resulting in overall octahedral bonding orbital geometry about the metal centre. The schematic structure (**1**) illustrates the three-fold rotation symmetry of the MB_{12} unit, and structure (**2**) the bonding disposition about the ruthenium centre.

We are not able to report details of the dimensions of the structure of this species of three-fold symmetry, as the compound has so far been reluctant to crystallize in a form suitable for single-crystal *X*-ray diffraction analysis. We have however been able to carry out such an *X*-ray analysis of the closely related species $[(PPh_3)_2ClRuB_{12}H_{11}(NEt_3)]$, which was obtained as air-stable red-orange crystals in 30% yield when the reaction was carried out with $[NHEt_3]_2[B_{12}H_{12}]$ and $[RuCl_2(PPh_3)_3]$ [equation (1)], rather than with the disodium salt and $[RuCl_3(PMe_2Ph)_3]$ as discussed above.

$$[RuCl_2(PPh_3)_3] + [NHEt_3]_2[B_{12}H_{12}] \longrightarrow [(PPh_3)_2ClRuB_{12}H_{11}(NEt_3)] + [NHEt_3]Cl + H_2 + PPh_3 \quad (1)$$

The stoicheiometry is now straightforward, and no change in formal ruthenium oxidation state is involved; the yield is correspondingly greater. Compared to the symmetrical species $[(PMe_2Ph)_3RuB_{12}H_{12}]$ [structures (**1**) and (**2**)], this second compound has a boron-bound NEt_3 group instead of an *exo*-bound hydride, and electroneutrality is maintained by the presence of a chloride ligand instead of one of the neutral phosphines on the metal centre [structure (**3**)].

The *X*-ray diffraction analysis showed that there was solid-state disorder in the boron-bound NEt_3 group which precluded the determination of cluster hydrogen-atom positions. It was however evident from n.m.r. spectroscopy (see later) that the metallaborane cluster had the expected eight *exo*-terminal and three bridging hydrogen atoms; electron-density maxima corresponding approximately to many of these positions appeared on Fourier difference maps but many did not refine to chemically plausible positions and all were therefore excluded in the refinement presented here. Selected interatomic distances

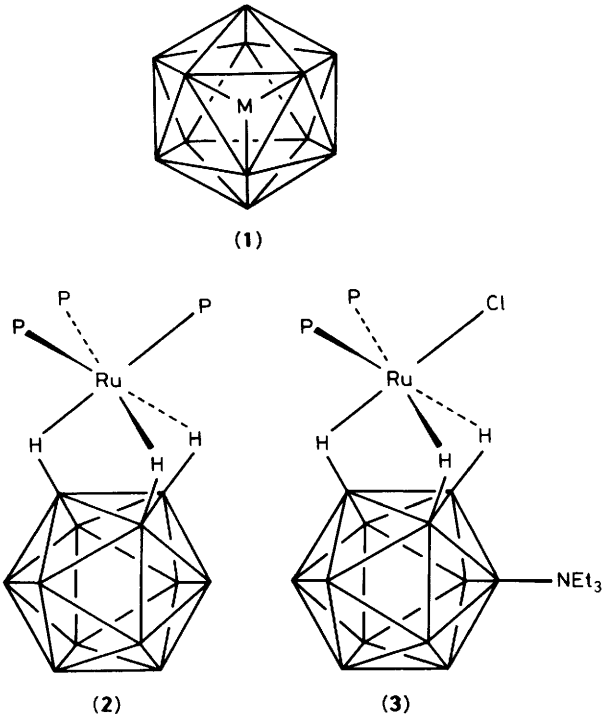

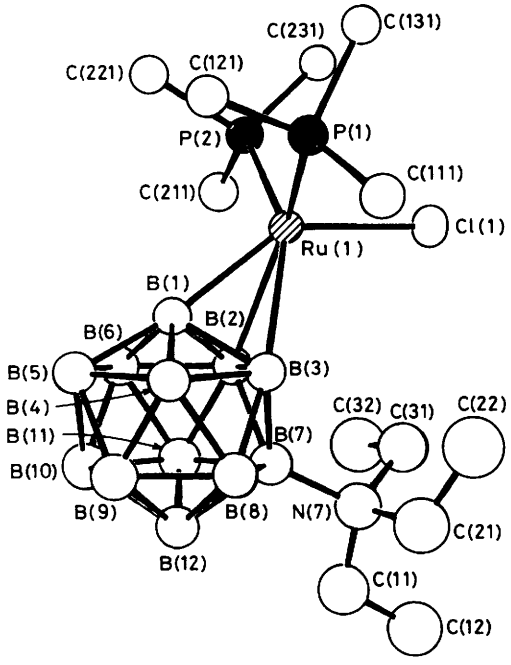

Figure 2. Molecular structure of $[(PPh_3)_2ClRuB_{12}H_{11}(NEt_3)]$. Hydrogen atoms were not located in this analysis, but n.m.r. spectroscopy (Table 4) shows *exo* terminal H atoms on all boron atoms except B(6), B(1), B(2), and B(3), and bridging H atoms between Ru and each of B(1), B(2) and B(3). Carbon atoms of PPh_3 other than the *ipso* ones are omitted for clarity while the N-ethyl group is shown in one of its two positions, again for clarity. The data were obtained on the 1:1 solvate with CH_2Cl_2

and angles are given in Tables 2 and 3 respectively, and the molecular structure in Figures 2 and 3.

The structure is seen to be based on a near-regular triangulated icosahedron of 12 boron atoms with the metal

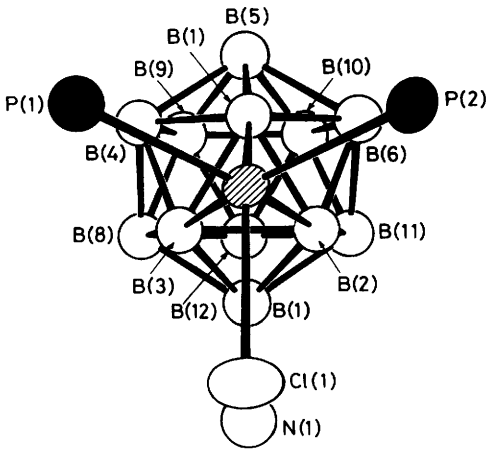

Figure 3. A view of the $P_2ClRuB_{12}N$ atoms of $[(PPh_3)_2ClRuB_{12}H_{11}(NEt_3)]$ chosen to illustrate the idealized mirror plane and the approximation to three-fold symmetry of the RuB_{12} grouping [compare structure (**1**)]

atom capping one of the triangular faces. The metal centre has three *exo*-polyhedral ligands (two phosphines and one chloride) approximately trigonally disposed about a three-fold icosahedral axis. The Cl–Ru–P and P–Ru–P interatomic angles at 96.5(2), 93.6(2), and 100.8(2)° are somewhat greater than the 90° expected for an ideal octahedral bonding-orbital disposition about the ruthenium atom. This has been observed in other metallaboranes with triphenylphosphine ligands (see, for example, refs. 10 and 11), and may arise from steric effects associated with the bulky P-phenyl groups and/or from the electronic and geometric constraints of the metal-to-borane bonding at the other side of the ruthenium atom. The *exo*-ligand bonding vectors are approximately *trans* to the vectors to the metal-bound boron atoms in the B(1)B(2)B(3) triangle, so that the two sets of three bonding vectors are in a mutually staggered configuration (Figure 3). The angles subtended at the metal atom by the atoms of this metal-bound boron triangle average at about 42°, but hydrogen atoms bound to them at idealized positions radial to the centre of the B_{12} cluster would subtend angles larger than these. Thus the electron-density maxima at these approximate positions in difference maps subtend angles of 82.6—93.3° (mean 87.5°) with each other and the other ruthenium-bound ligands which are *cis* to them, consistent with three-centre B–H–M bonding and a formal octahedral ruthenium(II) centre.

The (disordered) NEt_3 ligand is bound through nitrogen to the cluster boron atom B(7), in an eclipsed position relative to the ruthenium-bound chloride ligand; this converts the idealized three-fold skeletal symmetry of $[L_3RuB_{12}H_{12}]$ [structure (**1**) above] to an idealized mirror-plane skeletal symmetry for $[L_2ClRuB_{12}H_{11}L']$. Although there is no crystallographic mirror plane through the molecule, the configuration of the $P_2ClRuB_{12}H_{11}N$ unit approximates to this symmetry (Figure 3), and the n.m.r. properties discussed below (Table 4) show that in solution the cluster has the time-averaged mirror-plane symmetry that is expected from free rotation of the bonds to and within the phosphine and amine ligands. The intracluster electronic effect of the boron-bound amine ligand together with the differential *trans* effects of the metal-bound chloride and phosphine ligands result in asymmetry of the metal-to-borane bonding, so that the Ru–B(2) and Ru–B(3) distances, *trans* to phosphines and averaging *ca.* 247.5 pm, are somewhat longer than that to B(1), which is *trans* to chloride and *ca.* 227 pm. [Other measured ruthenium–boron distances in

Table 4. Selected n.m.r. parameters for $[(PPh_3)_2ClRuB_{12}H_{11}(NEt_3)]$ in CD_2Cl_2 solution at 21 °C[a]

δ(^{11}B)[b]	Relative intensity	δ(^{1}H)[c]	Relative intensity
+1.9[d]	1 B		
−13.2	2 B	+1.44	2 H
−14.5	1 B	+1.73	1 H
ca. −15 }	4 B[e]	+1.68	2 H
ca. −15 }		+0.26	2 H
−16.1	1 B	+0.88	1 H
−17.4[f]	1 B	−0.37[g]	1 H
−21.9[h]	2 B	−1.16[i]	2 H[j]

[a] δ(^{31}P) +58.2 p.p.m. ($CDCl_3$, −50 °C) relative to 85% H_3PO_4. [b] In p.p.m. ±0.5 to high field (low frequency) of $BF_3(OEt_2)$ in $CDCl_3$. [c] In p.p.m. ±0.05 to high field (low frequency) of $SiMe_4$ in $CDCl_3$; proton resonances related to directly bound borons by selective ^{1}H-{^{11}B} spectroscopy. [d] B(6) position; N-substituted. [e] Two accidentally coincident ^{11}B resonances (2 × 2 B) differentiated by their association with two different ^{1}H resonances. [f] B(3) position. [g] H(3) bridging atom. [h] B(1),B(2) positions. [i] H(1),H(2) bridging atoms; note no doublet structure arising from $^2J(^{31}P–Ru–^1H)$ (*trans*) resolved; coupling therefore ≤ *ca.* 10 Hz (contrast Table 1, footnote *e*). [j] $^1J(^{11}B–^1H)$ *ca.* 110 Hz; other couplings $^1J(^{11}B–^1H)$ not measurable due to overlapping resonances.

polyhedral metallaboranes range from 226(1) to 246.0(12) pm for Ru–H–B and from 203(11) to 251.7(9) pm for unbridged Ru–B,[5,7,8,12] but the data base is really too limited for a significant detailed comparison.] These ligand effects may also induce differential effects in the cluster interboron distances. For example B(1)–B(2) and B(1)–B(3) each appear to be some 3 pm shorter than B(2)–B(3), but magnitudes of the e.s.d.s associated with these indicate that these differences may not be statistically significant. Similar considerations arise when assessing these three apparently shorter interboron distances (which average *ca.* 174.5 pm) in relationship to the other cluster interboron distances (which average *ca.* 177.3 pm): although such shorter interboron distances within the ruthenium-bound triangular face would presumably be a consequence of contributions from multicentre RuB(1)B(2)B(3) bonding in addition to or at the expense of Ru–H–B bonding,[2] any such changes do not seem to be particularly marked. It may be noted at this point that the mutual similarity of all the intracluster interboron distances [range 173(2)—183(2) pm] obviously indicate that the metal atom has not *inserted* into the B_{12} cluster, but it is *exo* bound to it.

These general considerations are reflected in the measured n.m.r. properties (Table 4). The change to mirror-plane symmetry, compared to the compound of idealized C_{3v} symmetry (Table 1), is reflected in the change of the ^{11}B relative intensity pattern from 3:3:3:3 to 2:1:1:2:2:1:1:2, with corresponding changes of the relative intensities in the proton spectra. For both of the RuB_{12} species described in the present work there are no dramatic changes in ^{11}B chemical shifts compared with the anionic *closo* species $[B_{12}H_{12}]^{2-}$ and $[B_{12}H_{11}(NEt_3)]^-$. The most obvious difference is the shielding effect of up to *ca.* 9 p.p.m. for ^{11}B in the ruthenium-bound BH(1), BH(2), and BH(3) positions, and correspondingly in the proton spectrum there is a diagnostically higher shielding[9] for the B–H–Ru bridging hydrogen atoms. An interesting feature is that the magnitudes of the couplings $^1J(^{11}B–^1H)$ to the latter are only *ca.* 100 Hz. This value is markedly smaller than for free *exo*-terminal hydrogen atoms (which typically exhibit values of around 150 Hz) and markedly larger than for conventional *endo* B–H–M hydrogen atoms (which typically exhibit magnitudes of up to only a few tens of Hz). The reduction from the free *exo*-terminal value presumably arises from the effective conversion from two-centre to three-centre bonding, and as such it constitutes an important example in the assessment of the effects of multicentre bonding on simple expressions used to describe the Fermi-contact coupling mechanism.[9] A second interesting feature is the lower proton shieldings of these bridging hydrogen atoms in the substituted compound (Table 4) compared to the symmetrical unsubstituted species (Table 1). This could be a result of differential anisotropic neighbour shielding effects of the P-organyl groups of the phosphine ligands, or could also possibly reflect a looser bonding between the formal monoionic moieties $[RuCl(PPh_3)_2]^+$ and $[B_{12}H_{11}(NEt_3)]^-$ as compared to the formal di-ionic moieties $[Ru(PMe_2Ph)_3]^{2+}$ and $[B_{12}H_{12}]^{2-}$. The latter could also be reflected in the *ca.* 20 Hz difference in the couplings $^1J(^{11}B–^1H)$ for the Ru–H–B bridging hydrogen atoms in the two compounds.

The borane-to-metal bonding mode is of interest because it represents a new variation on established metallaborane structural themes, and the compounds also constitute the first examples of covalent metal complexes of a B_{12} ligand. Although dihapto bonding *via* two B–H–M bridging bonds from a B_2H_2 unit in the *closo*-$[B_{10}H_{10}]^{2-}$ anion is well established for copper,[1–3] and is also known for platinum,[4] no metal complexes of *closo*-$[B_{12}H_{12}]^{2-}$ and derivatives have previously been reported. The particular borane-to-metal binding mode, trihapto *via* three B–H–M bridging bonds from a B_3 triangle, is also novel for a *closo*-type binary borane ligand, although the bonding mode is well characterized, but not common, for more open formal binary borane ligands, as in the species $[(CO)_3MnB_3H_8]$[13] and $[(CO)_3MnB_8H_{13}]$.[14] Other related bonding modes are exhibited by the species $[(CO)_6BrMn_2B_3H_8]$[15] and $[(CO)_{10}HMn_3B_2H_6]$,[16] and a family of compounds represented by $[(PPh_3)_2ClRuClRu(PPh_3)B_{10}H_8(OEt)_2]$.[7] As with these other polyhapto B–H–M bridging modes, there is undoubtedly a contribution to the borane-to-metal bonding from direct metal–boron interaction,[2,5,17] although, as discussed above, geometrical and n.m.r. considerations show that this does not seriously perturb the *closo*-dodecaborate cluster character.

As an alternative to this metal–ligand co-ordination chemistry approach to the bonding,[5] the compounds may also be considered as 13-vertex metallaborane clusters. In this second approach the neutral $Ru(PMe_2Ph)_3$ centre is isoelectronic and isolobal in cluster terms with neutral BH, and so the species $[(PMe_2Ph)_3RuB_{12}H_{12}]$, taken as the example, is equivalent to the (as yet hypothetical) neutral borane $B_{13}H_{13}$ with a *pileo* 2*n* cluster-electron count. A geometry compatible with this *pileo* count is the 'capped *closo*' concave polyhedron,[18] in accord with the observed geometry (Figure 2), although in the present examples the localization of three cluster electron pairs in the three B–H–M bonds of the 'cap' results in a retention of the *closo*-dodecaborate character of the B_{12} residue. This last phenomenon exemplifies an important general consideration in polyhedral heteroborane species, namely that localization of electron density in particular sites can confer particular cluster character among the remaining cluster atoms; in extreme cases this can produce markedly different variations in cluster character within the framework of identical formal electron counts.[19,20]

It is of interest that, in these reactions of $[B_{12}H_{12}]^{2-}$, the integrity of the *closo* 12-vertex cluster is maintained, whereas with 10-vertex $[B_{10}H_{10}]^{2-}$ an effective oxidative insertion of the metal centre to give an 11-vertex metallaborane occurs [equation (2)].[6–8] This insertion of the metal centre into

$$[RuCl_2(PPh_3)_3] + [B_{10}H_{10}]^{2-} + 2EtOH \longrightarrow [(PPh_3)_2RuB_{10}H_8(OEt)_2] + PPh_3 + 2Cl^- + 2H_2 \quad (2)$$

$[B_{10}H_{10}]^{2-}$ is however accompanied by ethoxy-substitution of

the cluster, and presumably occurs *via* an initial *closo*-$[B_{10}H_{10}]^{2-}$ complex with the metal centre, analogous to the $[B_{12}H_{12}]^{2-}$ complex $[(PMe_2Ph)_3RuB_{12}H_{12}]$ reported here and to the previously reported $[B_{10}H_{10}]^{2-}$ complexes with copper[1-3] and platinum[4] centres. From this initial complex, metal insertion is probably induced by nucleophilic attack by ethanol on the cluster.[4] The isolation of the NEt_3-substituted species $[(PPh_3)_2ClRuB_{12}H_{11}(NEt_3)]$ from the B_{12} reaction shows that nucleophilic attack can also occur in this system, but that it does not then so readily induce an oxidative insertion of ruthenium into the cluster. This tendency to undergo substitution rather than cluster expansion is presumably at least partly a consequence of the inherently greater stability of the closed B_{12} *versus* the closed B_{10} cluster.

Experimental

The starting ruthenium complexes $[RuCl_2(PPh_3)_3]$[21] and $[RuCl_3(PMe_2Ph)_3]$[22] were prepared according to literature methods. Reactions were carried out, and solutions and solids generally stored, under dry nitrogen, although manipulations and separatory procedures were generally carried out in air. Preparative t.l.c. was carried out using silica gel G (Fluka, type GF254) on plates of dimensions 200 × 200 × 1 mm, made in these laboratories from an acetone slurry followed by drying in air at 100 °C. N.m.r. spectroscopy at 2.35 and 8.46 T was performed on JEOL FX-100 (University of Leeds) and Bruker WH-360 (S.E.R.C. Service, University of Edinburgh) instruments, respectively. The selective ^1H-$\{^{11}B\}$ experimental technique has been described elsewhere,[23-25] and ^{31}P spectra were recorded at low temperatures to maximize 'thermal decoupling' of the boron nuclei;[26] other n.m.r. spectroscopy was straightforward. Chemical shifts $\delta(^1H)$, $\delta(^{31}P)$, and $\delta(^{11}B)$ are given in p.p.m. to high frequency (low field) of Ξ100, Ξ40.480 730 (nominally 85% H_3PO_4), and Ξ32.083 971 MHz [nominally $BF_3(OEt_2)$ in $CDCl_3$][9] respectively.

Reaction between $[NHEt_3]_2[B_{12}H_{12}]$ *and the Complex* $[RuCl_2(PPh_3)_3]$.—A sample of $[NHEt_3]_2[B_{12}H_{12}]$ (200 mg, 0.58 mmol) was dissolved in refluxing ethanol (100 cm^3) and $[RuCl_2(PPh_3)_3]$ (556 mg, 0.58 mmol) was added. The mixture was heated under reflux for 3 h, then the ethanol was removed under reduced pressure (50—60 °C, rotary evaporator, water pump) and the resulting residue purified by preparative t.l.c. using CH_2Cl_2–n-C_5H_{12} (80:20) as eluting medium. This yielded $[(PPh_3)_2ClRuB_{12}H_{11}(NEt_3)]$ (R_f 0.3, 157 mg, 0.17 mmol, 30% yield), a bright orange solid, as the only identified metallaborane product. Recrystallization by diffusion of n-C_5H_{12} into a solution in CH_2Cl_2 yielded crystals of the 1:1 CH_2Cl_2 solvate suitable for *X*-ray diffraction analysis (see below). N.m.r. data are summarized in Table 4.

Reaction between $Na_2[B_{12}H_{12}]$ *and* $[RuCl_3(PMe_2Ph)_3]$.—A mixture of $Na_2[B_{12}H_{12}]$ (100 mg, 0.53 mmol) and $[RuCl_3(PMe_2Ph)_3]$ (330 mg, 0.53 mmol) was suspended in ethanol (150 cm^3) and heated under reflux for 1 h. The resulting bright red solution was reduced in volume (50—60 °C, rotary evaporator, water pump), and the residue then purified by preparative t.l.c. using CH_2Cl_2–n-C_5H_{12} (70:30) as eluting medium. This resulted in the isolation of $[(PMe_2Ph)_3RuB_{12}H_{12}]$ (R_f 0.9, 34

Table 5. Atomic co-ordinates (× 10^4) for $[(PPh_3)_2ClRuB_{12}H_{11}(NEt_3)]\cdot CH_2Cl_2$ with e.s.d.s in parentheses

Atom	*x*	*y*	*z*	Atom	*x*	*y*	*z*
Ru(1)	9 742(1)	1 487(1)	2 106(1)	C(232)	7 959(2)	1 997(4)	944(3)
P(1)	9 709(1)	3 391(2)	2 070(1)	C(233)	7 367(2)	2 109(4)	387(3)
P(2)	8 806(1)	1 095(2)	2 260(1)	C(234)	6 841(2)	1 517(4)	418(3)
Cl(1)	9 305(1)	1 199(2)	826(1)	C(235)	6 908(2)	814(4)	1 007(3)
C(111)	10 285(3)	3 856(5)	1 655(3)	C(236)	7 500(2)	702(4)	1 564(3)
C(112)	10 172(3)	3 626(5)	926(3)	B(1)	10 568(5)	992(9)	3 124(6)
C(113)	10 630(3)	3 899(5)	628(3)	B(2)	10 454(5)	−163(9)	2 556(5)
C(114)	11 202(3)	4 401(5)	1 059(3)	B(3)	10 873(5)	1 026(9)	2 428(6)
C(115)	11 315(3)	4 631(5)	1 788(3)	B(4)	11 334(5)	1 611(9)	3 284(6)
C(116)	10 857(3)	4 358(5)	2 086(3)	B(5)	11 179(5)	772(9)	3 965(6)
C(121)	9 952(3)	4 226(4)	2 918(3)	B(6)	10 632(5)	−373(9)	3 517(6)
C(122)	10 099(3)	3 729(4)	3 599(3)	B(7)	11 161(5)	−355(10)	2 351(6)
C(123)	10 251(3)	4 401(4)	4 218(3)	B(8)	11 696(6)	777(10)	2 790(6)
C(124)	10 255(3)	5 569(4)	4 156(3)	B(9)	11 896(6)	589(10)	3 754(6)
C(125)	10 108(3)	6 066(4)	3 475(3)	B(10)	11 481(6)	−620(10)	3 897(6)
C(126)	9 956(3)	5 395(5)	2 855(3)	B(11)	11 023(5)	−1 220(9)	3 034(6)
C(131)	8 958(2)	4 140(4)	1 584(3)	B(12)	11 793(6)	−627(9)	3 191(6)
C(132)	8 524(2)	4 171(4)	1 943(3)	N(7)	11 149(4)	−913(7)	1 591(5)
C(133)	7 928(2)	4 671(4)	1 610(3)	C(11A)	11 602(10)	−1 815(17)	1 725(10)
C(134)	7 766(2)	5 141(4)	919(3)	C(11B)	11 876(13)	−1 168(22)	1 704(14)
C(135)	8 200(2)	5 110(4)	561(3)	C(12A)	11 620(10)	−2 457(17)	1 059(11)
C(136)	8 796(2)	4 610(4)	893(3)	C(12B)	11 917(15)	−1 742(23)	997(16)
C(211)	8 762(3)	−424(4)	2 388(3)	C(21A)	11 449(10)	3(16)	1 152(11)
C(212)	8 697(3)	−878(4)	3 011(3)	C(21B)	10 752(12)	−383(20)	965(13)
C(213)	8 635(3)	−2 038(4)	3 069(3)	C(22)	11 032(7)	850(12)	817(7)
C(214)	8 638(3)	−2 743(4)	2 505(3)	C(31A)	10 484(9)	−1 099(15)	1 054(10)
C(215)	8 702(3)	−2 289(4)	1 883(3)	C(31B)	10 891(14)	−2 230(23)	1 570(16)
C(216)	8 764(3)	−1 129(4)	1 824(3)	C(32)	10 174(7)	−2 220(11)	1 308(7)
C(221)	8 707(3)	1 668(4)	3 077(2)	C(1S)	2 733(15)	1 752(24)	890(17)
C(222)	9 187(3)	1 467(4)	3 748(2)	Cl(1A)	2 299(5)	1 528(8)	1(6)
C(223)	9 123(3)	1 863(4)	4 384(2)	Cl(1B)	2 188(9)	2 049(16)	103(11)
C(224)	8 579(3)	2 461(4)	4 349(2)	Cl(1C)	2 383(10)	953(15)	3(10)
C(225)	8 099(3)	2 663(4)	3 679(2)	Cl(2A)	3 051(4)	131(8)	1 150(5)
C(226)	8 162(3)	2 266(4)	3 043(2)	Cl(2B)	3 005(8)	948(15)	1 563(10)
C(231)	8 026(2)	1 294(4)	1 533(3)	Cl(2C)	3 100(9)	959(16)	917(10)

mg, 0.052 mmol, 10% yield) as a lemon-yellow sparingly soluble solid (Found: C, 44.3; H, 6.9. $C_{24}H_{45}B_{12}P_3Ru$ requires C, 43.8; H, 6.8%). N.m.r. data are summarized in Table 1.

Crystallographic Studies.—All crystallographic measurements were made using an Enraf-Nonius CAD4 diffractometer operating in the ω–2θ scan mode using graphite-monochromatized Mo-K_α radiation (λ = 71.069 pm) in a manner described elsewhere in detail.[27] The structure was solved *via* standard heavy-atom procedures and refined using full-matrix least squares using the SHELX76 program system.[28] The ruthenium, phosphorus, and chlorine atoms were refined with anisotropic thermal parameters while all other atoms (including the triethylamine group which was found to be disordered over two positions) were refined with individual isotropic thermal parameters, the phenyl groups being treated as rigid groups with ideal hexagonal symmetry. A disordered CH_2Cl_2 molecule was also located in the Fourier difference map and this was treated in terms of interlocking CCl_2 triangles, each with an overall isotropic thermal parameter, which summed up to an occupancy of one. The weighting scheme $w = [\sigma^2(F_o) + g(F_o)^2]^{-1}$ was used at the end of refinement with parameter g varied so as to give acceptable agreement analyses. Final atomic co-ordinates and their standard deviations are given in Table 5.

Crystal data. $C_{42}H_{56}B_{12}ClNP_2Ru{\cdot}CH_2Cl_2$, M = 1 072.98, monoclinic, a = 2 246.3(2), b = 1 189.2(2), c = 1 972.5(2) pm, β = 111.04(1)°, U = 4.9176 nm^3, Z = 4, space group $P2_1/n$ (= $P2_1/c$, no. 14), D_c = 1.45 g cm^{-3}, μ(Mo-K_α) = 4.36 cm^{-1}, $F(000)$ = 1 908.

Data collection. Scan width $\omega = 0.8 + 0.35\tan\theta$, $3.0 < 2\theta < 44.0°$, scan speeds 1.35—6.77° min^{-1}. 6 551 Unique data, 4 636 observed [$I > 2.0\sigma(I)$].

Structure refinement. Number of parameters = 273, weighting factor g = 0.0005, R = 0.0626, R' = 0.0642.

Acknowledgements

We thank the S.E.R.C. for support and for a maintenance grant (to M. E.), Dr. D. Reed for services in n.m.r. spectroscopy, Professor H. Nöth (München) for a sample of $Na_2[B_{12}H_{12}]$, and Drs. M. B. Hursthouse and H. Dawes (Queen Mary College, University of London) for the crystallographic data collection.

References

1 R. D. Dobrott and W. N. Lipscomb, *J. Chem. Phys.*, 1962, **37**, 1779.
2 J. T. Gill and S. J. Lippard, *Inorg. Chem.*, 1975, **14**, 751.
3 R. K. Hertz, R. Goetze, and S. G. Shore, *Inorg. Chem.*, 1979, **18**, 2813.
4 Y. L. Gaft, Y. A. Ustynyuk, A. A. Borisenko, and N. T. Kuznetsov, *Zh. Neorg. Khim.*, 1983, **28**, 2234.
5 J. D. Kennedy, *Prog. Inorg. Chem.*, 1984, **32**, 519; 1986, **34**, 211.
6 J. E. Crook, M. Elrington, N. N. Greenwood, J. D. Kennedy, and J. D. Woollins, *Polyhedron*, 1983, **3**, 901.
7 M. Elrington, N. N. Greenwood, J. D. Kennedy, and M. Thornton-Pett, *J. Chem. Soc., Chem. Commun.*, 1984, 1398.
8 J. E. Crook, M. Elrington, N. N. Greenwood, J. D. Kennedy, M. Thornton-Pett, and J. D. Woollins, *J. Chem. Soc., Dalton Trans.*, 1985, 2407.
9 J. D. Kennedy, in 'Multinuclear N.M.R. (N.M.R. in Inorganic and Organometallic Chemistry),' ed. J. Mason, Plenum, London and New York, ch. 8, in the press and refs. therein.
10 N. N. Greenwood, J. D. Kennedy, W. S. McDonald, D. Reed, and J. Staves, *J. Chem. Soc., Dalton Trans.*, 1979, 117.
11 J. Bould, N. N. Greenwood, J. D. Kennedy, and W. S. McDonald, *J. Chem. Soc., Dalton Trans.*, 1985, 1843.
12 N. N. Greenwood, J. D. Kennedy, M. Thornton-Pett, and J. D. Woollins, *J. Chem. Soc., Dalton Trans.*, 1985, 2397.
13 S. J. Hildebrandt, D. F. Gaines, and J. Calabrese, *Inorg. Chem.*, 1978, **17**, 790.
14 J. C. Calabrese, M. B. Fischer, D. F. Gaines, and J. W. Lott, *J. Am. Chem. Soc.*, 1974, **96**, 6318.
15 M. W. Chen, D. F. Gaines, and L. G. Hoard, *Inorg. Chem.*, 1980, **19**, 2989.
16 H. D. Kaesz, W. Fellmann, G. R. Wilkes, and L. F. Dahl, *J. Am. Chem. Soc.*, 1965, **87**, 2753.
17 M. J. S. Dewar and M. L. McKee, *J. Am. Chem. Soc.*, 1976, **98**, 2086 and refs. therein.
18 R. Mason, K. M. Thomas, and D. M. P. Mingos, *J. Am. Chem. Soc.*, 1973, **95**, 3802.
19 J. Bould, Ph.D. Thesis, University of Leeds, 1983.
20 See, for example, M. A. Beckett, and J. D. Kennedy, *J. Chem. Soc., Chem. Commun.*, 1983, 575; M. Thornton-Pett, M. A. Beckett, and J. D. Kennedy, *J. Chem. Soc., Dalton Trans.*, 1986, 303.
21 P. S. Hallman, T. A. Stephenson, and G. Wilkinson, *Inorg. Synth.*, 1970, **12**, 237.
22 J. Chatt, G. J. Leigh, D. M. P. Mingos, and R. J. Paske, *J. Chem. Soc. A*, 1968, 2636.
23 J. D. Kennedy and B. Wrackmeyer, *J. Magn. Reson.*, 1980, **38**, 529.
24 J. D. Kennedy and N. N. Greenwood, *Inorg. Chim. Acta*, 1980, **38**, 93.
25 S. K. Boocock, N. N. Greenwood, M. J. Hails, J. D. Kennedy, and W. S. McDonald, *J. Chem. Soc., Dalton Trans.*, 1981, 1415.
26 J. D. Kennedy and J. Staves, *Z. Naturforsch., Teil B*, 1979, **34**, 808.
27 M. B. Hursthouse, R. A. Jones, K. M. A. Malik, and G. Wilkinson, *J. Am. Chem. Soc.*, 1979, **101**, 4128.
28 G. M. Sheldrick, SHELX76, Program System for *X*-ray Structure Determination, University of Cambridge, 1976.

Received 27*th March* 1986; *Paper* 6/614